Biophysical Chemistry 11 (1980) 339–343

POLYELECTROLYTE EFFECTS IN DNA CONDENSATION BY POLYAMINES

Victor A. BLOOMFIELD, Robert W. WILSON and Donald C. RAU
Department of Biochemistry, University of Minnesota, St. Paul, Minnesota 55108, USA

The conditions required for the counterion induced collapse of T7 bacteriophage DNA are briefly reviewed. Using Manning's counterion condensation theory we calculate a striking unity among collapse conditions: collapse occurs when from 89% to 90% of the DNA phosphate charges are neutralized by condensed counterions. The forces involved in collapsed DNA are investigated with emphasis on electrostatic repulsion. It is concluded that polyelectrolyte repulsion is the dominant force opposing collapse. Comparison of the results of polyelectrolyte repulsion calculation made using numerical methods and the Poisson–Boltzmann equation, with values of the attractive energies due to London dispersion interactions, leads to the conclusion that dispersion forces are probably large enough to cause collapse when the repulsions have been reduced by the presence of multivalent counterions.

1. Introduction

DNA is an extended, rigid molecule. What causes it to condense, so as to be packaged in virus capsids and chromosomes? What forces are involved? Polyelectrolyte repulsions are clearly the most important forces opposing condensation. While biological systems have probably developed special mechanisms, perhaps involving metabolic energy, to overcome these repulsions, it is interesting that condensation can be made to occur in simple test tube systems as well. Two major approaches have been developed. The first, termed ψ (psi, polymer and salt induced) condensation, requires high ionic strength to screen coulombic interactions and high concentrations of neutral polymer such as PEG to produce sufficient intermolecular excluded volume interactions to collapse the DNA [1,2]. The second, which we shall describe in this paper, requires polyamines to neutralize most of the DNA phosphate charge, after which attractive interactions between DNA segments are sufficient to cause spontaneous collapse [3–5].

In this paper we shall review experimental observations on polycation-induced condensation and how these may be systematized by counterion condensation theory, consider the balance between repulsive and attractive forces, and see how these factors may apply in packaging of DNA in bacterial viruses.

2. Polycation-induced condensation and charge neutralization

When a very dilute solution of T7 phage DNA in low ionic strength aqueous buffer is mixed with increasing amounts of spermidine, the DNA remains in solution as a flexible coil until a critical spermidine concentration is reached, when it spontaneously condenses into an extremely compact particle. Gosule and Schellman [3,4] observed the transition by flow dichroism, while we [5] have followed it by light scattering. Electron microscopy of the condensed DNA typically reveals toroidal particles, though sometimes spheres are observed [5,6]. The particles have hydrodynamic radii of about 500 Å, somewhat larger than the EM sizes when heavy metal stains were used, but in good agreement with EM sizes in the absence of stain. These sizes are comparable to the radius of the T7 phage capsid.

Condensation is a strongly cooperative process, occurring over a narrow range of polyamine concentration. For example, in a buffered solution containing 1 mM NaCl and 1 mM cacodylate, the light scattering intensity increases abruptly over the range 20–24 μM spermidine, then levels off. The critical spermidine concentration increases as $[Na^+]$ increases. If Mg^{2+} is used instead of Na^+, the concentration of spermidine required to cause collapse decreases. Spermine (a tetramine) causes collapse at a lower concentration than spermidine (a triamine). Putrescine or Mg^{2+}, both divalent

cations, do not themselves cause condensation in aqueous solution.

We have analyzed a great deal of this sort of data, using Manning's theory of counterion condensation [7]. In solutions containing only a single type of counterion of valence Z, counterion condensation theory predicts that the linear charge density of the polyion will be reduced by a factor

$$r = 1 - (Z\xi)^{-1}, \quad (1)$$

where $\xi = q^2/\epsilon k_B T b$, q is the proton charge, ϵ is the solvent dielectric constant, and b is the linear polyelectrolyte charge spacing in the absence of associated counterions. For DNA in H_2O at 20°, $b = 1.7$ Å, $\xi = 4.2$, and $r = 0.76, 0.88, 0.92$, and 0.94 for mono-, di-, tri-, and tetravalent counterions.

When there is a mixture of counterions of different valences, matters are more complicated. We have slightly modified Manning's treatment [7] to obtain the simultaneous equations

$$1 + \ln(1000\theta_1/c_1 V_{P1}) = -2Z_1\xi(1 - Z_1\theta_1 - Z_2\theta_2)\ln(1 - e^{-\kappa b}), \quad (2)$$

$$\ln(\theta_2/c_2) = \ln(V_{P2}/1000e) + (Z_2/Z_1)\ln(1000\theta_1 e/c_1 V_{P1}), \quad (3)$$

where θ_1, θ_2 are the fractions of bound ions, V_{P1} and V_{P2} the volumes in which they are bound, c_1 and c_2 their concentrations, and κ is the Debye-Hückel screening parameter. Iterative solution of these equations leads finally to the fraction of DNA phosphate charges neutralized,

$$r = Z_1\theta_1 + Z_2\theta_2. \quad (4)$$

This analysis reveals a remarkable regularity. Regardless of the relative amounts of spermidine or spermine to Mg^{2+} or Na^+, DNA condensation occurs when $r = 0.89$ to 0.90. Thus the determining factor in collapse is not the ratio of bound polyamine to DNA phosphate, but rather the neutralization of 89–90% of the phosphate charge.

Inspection of eq. (1) and the definition of ξ suggests that r could be increased, for a given Z, by lowering the dielectric constant. We tested this idea by studying DNA condensation in a 50% water-methanol mixture, whose dielectric constant is 60 rather than 80 for pure water. This gives $\xi = 5.6$, and $r = 0.82, 0.91, 0.94$, and 0.96 for mono-, di-, tri-, and tetravalent ions. If $r \geq 0.89$ is required for DNA condensation, then divalent cations should suffice. Experiments with Mg^{2+} and with putrescine confirmed this prediction. We also found, as expected, that less spermidine was required for condensation in H_2O–MeOH than in aqueous solution alone.

3. Balance of repulsive and attractive forces

In order to condense DNA into a compact toroid or sphere, unfavorable free energy factors associated with bending, elastic entropy, and electrostatic repulsion must be overcome. A similar problem was addressed by Riemer and Bloomfield [9] who estimated the contributions to the free energy from bending, entropy of condensation, and polyelectrolyte repulsion for the packaging in the capsid of T4 phase DNA. Using their equations, we have calculated these values for two smaller viral DNA's as well, λ and T5. In each case we assumed a capsid thickness of 35 Å, a DNA persistence length of 650 Å, a hydrated diameter of 25 Å, and $T = 293$°K. Phages λ and T5 have isometric capsids, with outer radii of 330 Å and 450 Å, while T4 is a prolate icosehedron, 565 × 445 Å. Unhydrated DNA occupies 41 to 46% of the internal head volume in each case. Free energies are listed in table 1 in kcal/mol virus.

These values show that polyelectrolyte repulsion, ΔG_{elec}, is by far the dominant thermodynamic barrier to packaging of DNA within viruses. We therefore focus our attention on the electrostatic opposition to DNA collapse using a numerical solution of the Poisson–Boltzmann equation for a charged cylinder surrounded by identical cylinders, in a regular array.

We begin with the general form of the Poisson–Boltzmann equation for the potential $\psi(r)$ at position r in solution:

$$\nabla^2\psi = -\frac{4\pi}{\epsilon}\sum_i Z_i q c_i \exp(-Z_i q\psi/k_B T), \quad (5)$$

where qZ_i is the charge on ionic species i, and c_i is the concentration in ions/cm^3. Introducing the molar concentration C_i, Debye–Hückel shielding parameter $\kappa = (8\pi N_A q^2/1000\epsilon k_B T)^{1/2} I^{1/2}$, the ionic strength $I = \frac{1}{2}\Sigma_i C_i Z_i^2$, the reduced potential $\phi = q\psi/k_B T$, this becomes

Table 1
Calculated contributions to the free energy of packaging DNA inside three bacterial viruses

Bacteriophage	λ	T5	T4
DNA mol wt × 10^{-6}	31	75	110
≒ coaxial coils within head	8.6	9.8	9.5
ΔG_{bend}, kcal/mol	1.1×10^3	9.7×10^2	1.4×10^3
ΔG_{cond}, kcal/mol	1.4×10^2	3.5×10^2	5.1×10^2
ΔG_{elec}, kcal/mol	5.7×10^4	1.4×10^5	2.1×10^5

$$\nabla^2\phi = -\frac{1}{2}\frac{\kappa^2}{I}\sum_i Z_i C_i \exp(-Z_i\phi) . \quad (6)$$

In cylindrical coordinates, where

$$\nabla^2 = \partial^2/\partial\rho^2 + (1/\rho)\,\partial/\partial\rho ,$$

if there is no angular dependence of the potential, we define the reduced distance $x = \kappa\rho$ and let $z = \ln x$, finally arriving at

$$\frac{\partial^2\phi(z)}{\partial Z^2} = -\frac{e^{2z}}{2I}\sum_i Z_i C_i \exp\{-Z_i\phi(z)\} . \quad (7)$$

This equation is to be solved by Runge–Kutta numerical integration, given the proper boundary conditions.

The potential is constant inside the insulating rod, so the boundary condition at the surface is

$$\partial\psi/\partial\rho|_{\rho=a} = -4\pi\sigma/\epsilon , \quad (8)$$

where a is the radius of the cylinder and σ is the surface charge density $Z_p\sigma/2\pi a$. The linear charge density is Z_p. In the reduced variables defined above,

$$\partial\phi/\partial z|_{z=\ln\kappa a} = -2q^2 Z_p/\epsilon k_B T = -2\xi . \quad (9)$$

This boundary conditions holds for both an isolated rod and an array of nearby rods. The boundary conditions far from the rod surface are different, however.

For an isolated rod, we can move far enough away that the linearization approximation

$$\exp(Z_i\phi) = 1 + Z_i\phi , \quad (10)$$

will be accurate. The solution to this in the limit $x \to \infty$ is well known to be

$$\phi(x) = cK_0(z) , \quad (11)$$

with first derivative

$$\partial\phi/\partial x = -cK_1(x) , \quad (12)$$

where K_0 and K_1 are modified Bessel functions.

Eliminating the normalization constant c, and transforming variables from x to z, we obtain

$$\partial\phi/\partial z = -e^z\phi(z)K_1(z)/K_0(z) . \quad (13)$$

Our numerical integration strategy is then to pick a very small reduced potential, in the neighborhood $\phi = 10^{-4}$, and a starting value of z, then run through a Runge–Kutta integration of eq. (13) to determine $\partial\phi/\partial z$ at the surface. If this is not within 0.1% of the value required by eq. (9), we systematically vary the starting z until agreement is obtained.

In an extensive array of parallel, equally spaced rods, a different boundary condition applies. Halfway between any two rods the potential will be a minimum, corresponding to equally balanced electrical forces perpendicular to the normal plane betwen the two rods. We then assume that we can approximate the polygonally-shaped minimum potential surface surrounding any rod by a circular one with radius $R/2$, where R is the center-to-center distance between nearest neighbor rods. At this distance,

$$(\partial\phi/\partial z)_{z=\ln\kappa R/2} = 0 . \quad (14)$$

Then the only variable is ϕ at $R/2$, which is varied systematically as a starting value for Runge–Kutta integration inward toward the rod surface until eq. (9) is satisfied to within 0.1%.

As a check on our calculations, we can treat the Poisson–Boltzmann equation (eq. 7) as an inhomogeneous differential equation. If $\phi_{RK}(z)$ is the potential generated at z by the Runge–Kutta method, and $\phi(z)$ are the test potentials, then we should have

$$\partial^2\phi_T/\partial z^2 = -\frac{e^{2z}}{2I}\sum_i Z_i C_i \exp(-Z_i\phi_{RK}) . \quad (15)$$

For an isolated rod, integration by parts gives

$$\phi_T(z) = -\int_z^\infty (t-z)\frac{e^{2t}}{2I}$$

$$\times \sum_i Z_i C_i \exp\{-Z_i \phi_{RK}(t)\}\, dt\,, \qquad (16)$$

while for an array of rods

$$\phi_T(z) = -\int_Z^{\ln(\kappa R/2)} (t-z)\frac{e^{2t}}{2I}$$

$$\times \sum_i Z_i C_i \exp\{-Z_i \phi_{RK}(t)\}\, dt + \phi_{RK}(\kappa R/2)\,. \qquad (17)$$

If the potentials have been calculated properly, numerical integration should give $\phi_T(z) = \phi_{RK}(z)$ to within a fraction of a percent. This was always the case.

Once the potentials have been determined as a function of position, they can be used to compute the free energy. The most widely used method involves calculating the reversible work of charging the system and equating this to the ΔG of charging. Oosawa [9] has described an equivalent method whereby the internal energy

$$U_e = \int_V (\epsilon/8\pi)(\nabla\psi)^2 dV\,, \qquad (18)$$

and the entropy

$$S = -k \int_V \sum_i C_i [\ln(C_i/C_0) - 1]\, dV\,, \qquad (19)$$

are calculated separately and combined to give

$$G = U_e - TS\,. \qquad (20)$$

The local concentration of ionic species i in the volume element dV is related to the bulk concentration, $\bar{C}_i$, and the potential by

$$C_i = \bar{C}_i \exp(-Z_i q\psi/kT)\,, \qquad (21)$$

and C_0 is the concentration of solvent.

We use this method since it requires that the potentials be calculated only for the fully charged rods, thus significantly reducing the required computation time.

Performing these calculations for the isolated rod, $G(\infty)$, and for a rod surrounded by others at R, $G(R)$, we calculate the electrostatic work $\Delta G(R) = G(R) - G(\infty)$ required to form the condensed array.

Table 2
Differential electrostatic free energy for critical collapse conditions

Salt conditions	aqueous solution + 3 ions	$\Delta G_0(k_BT/PO_4)$ $R = 30$ Å	$R = 50$ Å
2.0×10^{-3} M + 1 ion	2.4×10^{-5} M	0.350	0.225
1.0×10^{-2} M + 1 ion	2.0×10^{-4} M	0.308	0.170
2.0×10^{-2} M + 1 ion	4.9×10^{-4} M	0.287	0.138
5.0×10^{-2} M + 1 ion	1.9×10^{-3} M	0.240	0.078
1.0×10^{-3} M + 2 ions	1.1×10^{-4} M	0.301	0.159
1.0×10^{-2} M + 2 ions	1.1×10^{-3} M	0.237	0.078
	+ 4 ions		
5.0×10^{-2} M + 1 ion	3.4×10^{-5} M	0.309	0.142
1.0×10^{-2} M + 2 ions	3.5×10^{-5} M	0.260	0.097
	50:50 MeOH:H_2O + 3 ions		
2.0×10^{-2} M + 1 ion	3.0×10^{-5} M	0.386	0.202
	+ 2 ions		
2.0×10^{-3} M + 1 ion	6.5×10^{-4} M	0.407	0.208
5.0×10^{-3} M + 1 ion	1.1×10^{-3} M	0.399	0.190
2.0×10^{-2} M + 1 ion	2.9×10^{-3} M	0.373	0.137

4. Results

In table 2 are listed a number of such calculated changes in electrostatic free energy. The calculations correspond to ionic conditions which we have found experimentally to cause DNA collapse [5]. Values are presented for two different inter-helical spacings, 30 Å and 50 Å, representing the minimum and maximum spacings thought consistent with x-ray scattering, electron microscopy and hydrodynamic measurements on condensed DNA's. The calculated repulsive free energies (in units of k_BT/PO_4) range from 0.237 to 0.407 at 30 Å spacing and 0.078 to 0.225 at 50 Å. These values can be compared with calculated values of 1.739 at 30 Å or 1.018 at 50 Å for a solution that is 2×10^{-3} M in monovalent cations and contains no higher valent cations. It is clear that the multivalent cations are important in causing large reductions in the repulsive energies, even if present only in micromolar concentrations.

The attractive force for condensation is presumably electrostatic and electrodynamic in origin, involving London dispersion forces and dipole-induced dipole

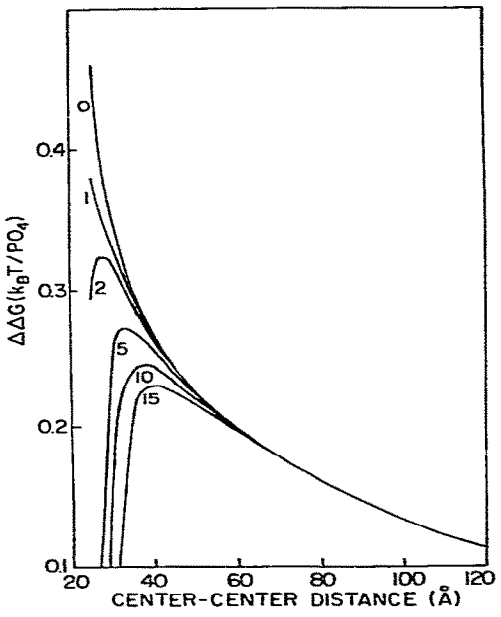

Fig. 1. Calculated net free energy of approach of two DNA double helices, as a function of center-to-center distance, in units of k_BT/phosphate. The numbers on the curves list the assumed value of the Hamaker constant A/k_BT. Ionic conditions for this calculation were 2×10^{-3} M + 1, 2.4×10^{-5} M + 3 and 2.072×10^{-3} M − 1 ions.

interactions. These forces are quite weak at long range but increase rapidly as the rods approach one another, with the attractive energy changing approximately as $1/R^5$. The strength of the dispersion forces is proportional to the empirical Hamaker constant A, whose magnitude for ordinary organic molecules interacting in water is $\sim 4 \times 10^{-14}$ erg; that is, about $|k_BT|$ at room temperature.

In fig. 1 we have plotted the sum of the repulsive and attractive free energies relative to a single isolated DNA helix as a function of R, for various choices of A (in units of $|k_BT|$ per phosphate) for a representative set of ionic conditions. In this instance we have calculated the attractive free energies using the method of Brenner and McQuarrie [10]. This method takes into account the finite radius of the rods, which causes the attraction to increase at a rate faster than $1/R^5$ as the rods get very close together.

Examination of fig. 1 reveals that in order for a net attraction at separation of around 30 Å to result, values of A of from 2 to 5 k_BT must be assumed. From optical data, Parsegian and Brenner [11] estimated a value of A for tobacco mosaic virus of from 1 to 2 k_BT. The possibility of dipole-induced dipole interactions in DNA can easily double the effective attraction.

Thus it appears that the polyamine-induced condensation of T7 DNA *in vitro* is akin to destabilization and flocculation of a colloidal suspension by adsorption of counterions on the surface of the colloidal particles. When the surface charge density is lowered sufficiently by association of counterions, particularly polyvalent ions, dispersion forces equal and then overweigh electrostatic repulsions and flocculation or condensation ensues.

Acknowledgements

This research was supported in part by NIH Grant GM 17855. D.C.R. was the recipient of a Dr. Chaim Weizmann Postdoctorate Fellowship for Scientific Research.

References

[1] L.S. Lerman, Proc. Nat. Acad. Sci. U.S.A. 68 (1971) 1886.
[2] Yu.M. Evdokimov, A.L. Platonov, A.S. Tikhonenko and Ya.M. Varshavsky, FEBS Lett. 23 (1972) 180.
[3] L.C. Gosule and J.A. Schellman, Nature 259 (1976) 333.
[4] L.C. Gosule and J.A. Schellman, J. Mol. Biol. 121 (1978) 311.
[5] R.W. Wilson and V.A. Bloomfield, Biochemistry 18 (1979) (1979) 2192.
[6] D.K. Chattoraj, L.C. Gosule and J.A. Schellman, J. Mol. Biol. 121 (1978) 327.
[7] G.S. Manning, Quart. Rev. Biophys. 11 (1978) 179.
[8] S.C. Riemer and V.A. Bloomfield, Biopolymers 17 (1978) 785.
[9] F. Oosawa, Polyelectrolytes (M. Dekker, New York, 1971).
[10] S.L. Brenner and D.A. McQuarrie, Biophys. J. 13 (1973) 301.
[11] V.A. Parsegian and S.L. Brenner, Nature (1976) 632.